Theor Chem Account (2008) 119:107–111
DOI 10.1007/s00214-006-0233-y

REGULAR ARTICLE

Protein voltammetry and spectroscopy: integrating approaches

Louise Male · Sophie J. Marritt · Ben C. Berks · Myles R. Cheesman · Jessica H. van Wonderen · Simon J. George · Julea N. Butt

Received: 5 September 2006 / Accepted: 8 November 2006 / Published online: 9 January 2007

Abstract Cyclic voltammetry readily visualizes the redox properties of many proteins. Net electron exchange between the protein and an electrode produces an electrical current that simultaneously quantitates and characterizes the underlying redox event(s). However, no direct information regarding the molecular origin, or consequences, of electron transfer is available. Integrating voltammetric and spectroscopic methods is one route to a more 'holistic' description of protein electron transfer. Here, we illustrate this approach with spectroelectrochemical studies of *Rhodovulum sulfidophilum* cytochrome c_2 and *Escherichia coli* cytochrome *bd* that employ electronic absorbance, infra-red and magnetic circular dichroism spectroscopies.

Keywords Cytochrome c_2 · Cytochrome *bd* · Infrared spectroscopy · Magnetic circular dichroism spectroscopy · Spectroelectrochemistry

L. Male · S. J. Marritt · M. R. Cheesman · J. H. van Wonderen · J. N. Butt (✉)
Centre for Metalloprotein Spectroscopy and Biology,
School of Chemical Sciences and Pharmacy,
University of East Anglia, Norwich Research Park,
Norwich, NR4 7TJ, UK
e-mail: j.butt@uea.ac.uk

B. C. Berks
Department of Biochemistry, University of Oxford,
South Parks Road, Oxford, OX1 3QU, UK

S. J. George
Physical Biosciences Division, Lawrence Berkeley National Laboratory, Berkeley, CA 94720, USA

J. N. Butt
Centre for Metalloprotein Spectroscopy and Biology,
School of Biological Sciences, University of East Anglia,
Norwich Research Park, Norwich, NR4 7TJ, UK

1 Introduction

Proteins that perform long-range electron transfer (ET) hold a particular fascination for scientists from a range of disciplines. The reasons for this are not difficult to see. The 'pure' ET event has an apparent simplicity whose application to proteins attracts much discussion [1]. There is also a considerable challenge to understand, and mimic by rationale design, the action of proteins that couple long range ET to ion transfer, conformational change and/or chemical transformation [2]. Additionally, the mechanisms that govern the regulated, integrated operation of ET proteins within the complex electronic and metabolic circuitry of a living cell have yet to be fully disclosed.

Fortunately, there are a number of techniques for studying and quantitating ET. In one, dynamic electrochemistry, the protein of interest forms part of an electrical circuit [3,4]. Electrons are exchanged between the protein and an electrode either directly or 'mediated' by low molecular weight redox molecules. In either case, this electron exchange is quantitated as a flow of electrical current that may provide insights into each of the topics above since the protein may be studied in isolation, as part of a multi-protein complex or in a cell [3–11].

When direct protein:electrode communication is studied by cyclic voltammetry the ET process is readily visualized. The applied electrode potential is varied in a 'saw tooth' fashion and the resultant current recorded at each potential. A single, reversible redox process produces a pair of peaks, of equal height, centered on the reduction potential. The peak of negative current seen on lowering the electrode potential reflects protein reduction. The peak of positive current on returning to positive potentials reflects protein oxidation.

Additional processes alter the current-potential profile, the voltammogram, in an intuitive way. Gated ET is reflected in an asymmetry of the peaks. Additional redox events produce additional peaks. At potentials where catalytic reduction (or oxidation) occurs a continuous flow of current is observed as electrons move from the electrode to molecules in solution (or vice versa) via the enzyme of interest. To understand the origin of these currents at a molecular level requires additional information. Specifically, structural and/or spectroscopic data are sought that describe changes occurring within the protein on traversing the potential range of interest. Samples may be poised chemically, or electrodically, at key potentials and transferred to an appropriate spectrometer. Alternatively, samples of defined but variable potential may be prepared in situ through the integration of spectroscopic and electrochemical methodologies. Here we illustrate the latter approach with spectroelectrochemistry of two proteins, *Rhodovulum sulfidophilum* cytochrome c_2 and *Escherichia coli* cytochrome *bd*.

2 Materials and methods

Cytochrome c_2 was purified from the periplasmic fraction of *R. sulfidophilum* grown photolithotrophically with thiosulfate as electron donor. Conditions for cell culture, subcellular fractionation and an initial purification by ion exchange chromatography were as described previously [12]. The cytochrome c_2 containing fractions from the ion exchange column were further refined by hydrophobic interaction and gel filtration chromatography. Cyclic voltammetry under conditions of semi-infinite diffusion was performed with a three electrode cell configuration utilizing a pyrolytic graphite 'edge' working electrode [11]. Electronic absorption and FTIR spectroscopies were performed in an OTTLE cell based on the design of Moss et al. [13]. MOTTLE experiments were as described in Marritt et al. [14]. FTIR spectroscopy and data analysis were performed as described previously [15].

3 *Rhodovulum sulfidophilum* cytochrome c_2

Bacterial cytochromes c_2 are periplasmic proteins that contain a single covalently bound heme with His-Met axial ligands [16,17]. Cytochrome c_2 from *R. sulfidophilum* returns electrons to the photosynthetic reaction center from the cytochrome bc_1 complex but it may also participate in thiosulfate oxidation during photolithotrophic growth with thiosulfate as electron donor [12,18].

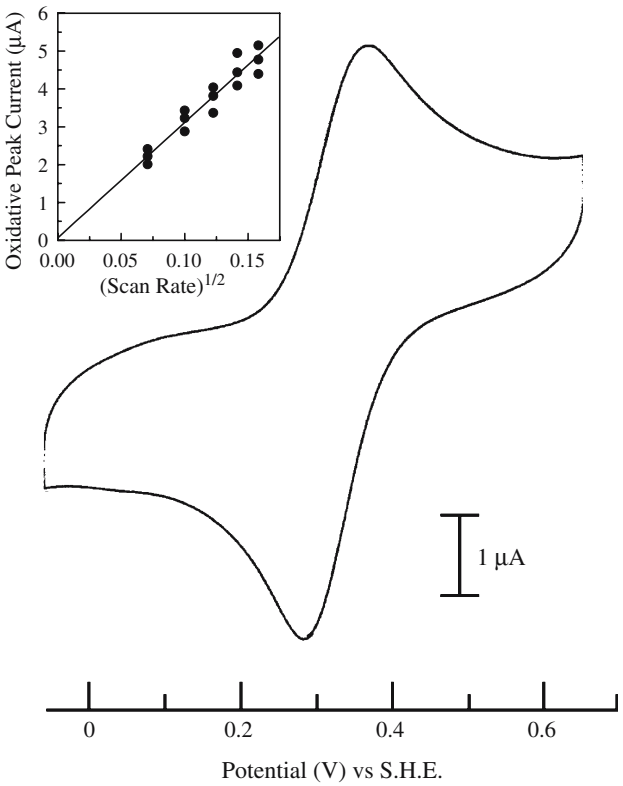

Fig. 1 Typical cyclic voltammogram of *R. sulfidophilum* cytochrome c_2 (1 mM protein, 15 mV s^{-1}) under semi-infinite diffusion conditions. Inset: Variation of oxidative peak current with scan rate (V s^{-1}). Buffer-electrolyte 10 mM Tris–HCl, pH 8.0, 4°C

Figure 1 shows a typical cyclic voltammogram of *R. sulfidophilum* cytochrome c_2 measured under conditions of semi-infinite diffusion. A pair of peaks are resolved that reflect direct electron exchange between cytochrome c_2 and the pyrolytic graphite 'edge' electrode used in this study. Reversible electron transfer is reflected in the equal heights of the oxidative and reductive peaks. From the average peak position a reduction potential of 315 ± 20 mV, pH 8 is calculated. The peak heights are in direct proportion to the square root of the voltammetric scan rate, Fig. 1 inset. This demonstrates that the voltammetry is determined by planar diffusion of the protein to, and from, the electrode. Under these conditions the peak separation of 65 ± 5 mV at 5 mV s^{-1} is consistent with the expected, reversible single electron transformation of the heme, $Fe^{3+/2+}$, center.

The molecular origin of the wave pair was confirmed by spectroelectrochemistry. A sample of *R. sulfidophilum* cytochrome c_2 was placed in an optically transparent thin layer electrochemical (OTTLE) cell with Perspex windows and a path length of ca. 90 μm. Gold mesh

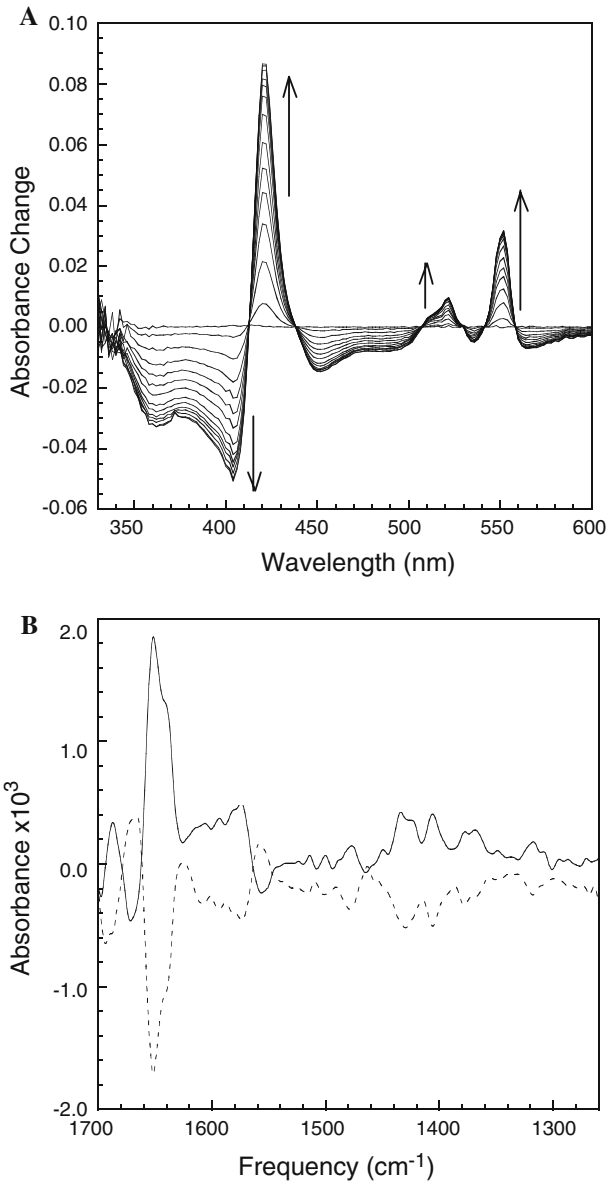

Fig. 2 Spectroelectrochemistry of *R. sulfidophilum* cytochrome c_2. **a** Change of electronic absorbance spectrum during reduction of cytochrome c_2. Potential stepped from 0.6 to −0.05 V versus SHE. Spectra collected at 7.5 s intervals. *Arrows* indicate changes with time. **b** Oxidized minus reduced (oxidation, *solid line*) and reduced minus oxidized (reduction, *broken line*) FTIR difference spectra of cytochrome c_2. Potential stepped from 0.6 to −0.05 V versus SHE for reduction and vice versa for oxidation. In both experiments the protein concentration was 0.4 mM in 10 mM Tris–HCl, D_2O, pH* 8.4, 25°C

coated with mercaptopropionic acid served as the working electrode. The sample equilibrated at 0.6 V displayed a spectrum typical of low-spin ferric heme. On stepping to 0.05 V significantly increased intensities were seen at 421, 520 and 552 nm with a number of isosbestic points between 400 and 600 nm, Fig. 2a. The spectral changes are typical of a ferric to ferrous transition at a low-spin heme. Comparison of the spectral changes with those observed on chemical (dithionite) reduction of the sample confirmed that complete reduction had occurred (data not shown). The spectral changes noted in the OTTLE cell were fully reversed when the potential was returned to 0.6 V and the protein equilibrated in the oxidized state.

The spectral information on changes at the heme (porphyrin core) can be complemented by information on the heme peripheral groups, protein side chains and backbone through FTIR redox difference spectra. For *R. sulfidophilum* cytochrome c_2 this was achieved by fitting the OTTLE cell with CaF_2, as opposed to Perspex, windows. The redox difference FTIR spectra for oxidation and reduction are mirror images of one another, Fig. 2b. Thus, the FTIR and optical spectra indicate reversibility of all the redox driven processes.

A full discussion of the redox difference FTIR spectra is beyond the scope of this paper. However, the behavior of *R. sulfidophilum* cytochrome c_2 can be readily compared with that of eukaryotic cytochromes *c* from comparable experiments. Moss et al. [13] showed that the redox difference FTIR spectra of seven eukaryotic cytochromes *c* were strikingly similar throughout the region 1,200–1,800 cm^{-1}. They suggested that the mechanistically important structural changes arise from highly conserved structural features. For example, a prominent, sharp derivative centered on 1,516 cm^{-1} in H_2O (1,514 cm^{-1} in D_2O) was attributed to a change in the environment around a tyrosine side chain. The molecular origin was suggested to be movement of the tyrosine positioned in proximity to the methionine axial-heme ligand as identified in crystallographic studies of oxidized and reduced cytochromes *c* [19].

The redox difference FTIR spectrum of *R. sulfidophilum* cytochrome c_2 lacks a prominent or sharp feature at ∼1,515 cm^{-1}. Indeed, there are relatively few similarities between the difference spectrum of *R. sulfidophilum* cytochrome c_2 and those of the cytochromes *c*. We note that the redox difference spectrum of horse heart cytochrome *c* reported by Moss et al. has been reproduced by a number of researchers [20,21] and by us (not shown). Thus, it appears that despite the overall structural homology predicted for the cytochromes *c* and c_2 they display distinct responses to a change of redox state.

4 *Escherichia coli* Cytochrome *bd*

Hemes are versatile cofactors. Their redox chemistry is exploited in proteins such as cytochrome c_2 that shuttles electrons between proteins. Their ability to exchange

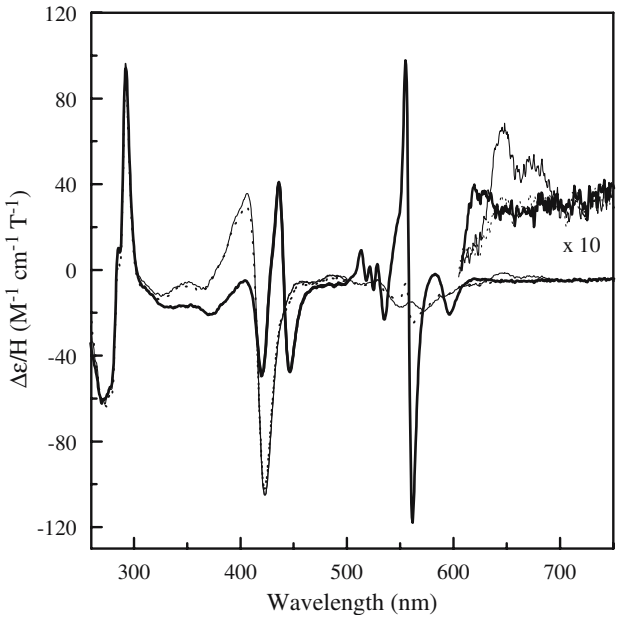

Fig. 3 MCD spectra of *E. coli* cytochrome *bd* (40 μM) equilibrated at defined potentials by MOTTLE. Sample 'as prepared' equilibrated at +325 mV (*light solid line*) after equilibration at +100 mV (*heavy solid line*) and then after equilibration at +348 mV (*broken line*). Buffer-electrolyte was 20 mM Hepes, 1 mM EDTA, 50 mM NaCl, pH 7.0. Reproduced with permission from Marritt et al. [14]

axial ligands is exploited in enzymes such as *E. coli* cytochrome *bd*, a membrane spanning heterodimer containing one *d*-type and two *b*-type hemes [22]. This respiratory oxidase uses reducing equivalents from quinol to catalyze the reduction of O_2. In as prepared enzyme, heme *d* is a mixture of ferryl ($Fe^{IV} = O$) and ferrous-oxy ($Fe^{II} - O_2$) forms that presumably reflect intermediates in O_2 reduction. Heme b_{558} has histidine and methionine as axial ligands and is proposed to play a direct role in quinol oxidation. Heme b_{595} is high-spin with histidine as one axial ligand and its role within enzyme is still a matter of debate.

We have seen how electronic absorption spectroscopy of cytochrome c_2 at visible wavelengths provides information on heme oxidation state. However, such spectra provide relatively little chemical information and they can fail to resolve signals from individual sites in multiheme proteins. When such information is required magnetic circular dichroism (MCD) spectroscopy can be a useful analytical tool [23–25]. The differential absorption of left- and right-circularly polarized light induced by the presence of a longitudinal magnetic field provides spectra that define heme oxidation-state, spin- and ligation-state in solution samples. Some of these features are illustrated in the MCD spectrum of as prepared cytochrome *bd*, Fig. 3. The dominant derivative centered on 414 nm arises from low-spin heme b_{558}. Smaller features are resolved between 460 and 600 nm that reflect overlapping contributions from both low- and high-spin ferric hemes. At longer wavelengths, peaks at 650 and 680 nm are assigned to ferrous-oxy ($Fe^{II} - O_2$) and oxo-ferryl ($Fe^{IV} = O$) forms of heme *d* respectively.

We have not yet achieved direct voltammetry of cytochrome *bd*. However, effective electrical communication between the enzyme and a gold mesh electrode is achieved in the presence of a mediator cocktail. By incorporating this configuration in an MCD-compatible OTTLE (MOTTLE) cell it has proved possible to poise an anaerobic sample of cytochrome *bd* at defined potentials in the MCD instrumentation and so monitor chemical changes at heme *d* [14].

On taking the as prepared enzyme from +325 to +100 mV in situ, considerable reduction of heme b_{558} is reflected in the emergence of an intense and sharp derivative centered on 558 nm. The small, broad derivative centered on 595 nm indicates the presence of high-spin ferrous heme b_{595}. Features characteristic of ferrous-oxy or oxo-ferryl heme *d* are not detected at longer wavelengths. Instead, a broad feature spanning ca. 620–630 nm is resolved that is likely to originate from ferrous heme *d*. Reoxidation of the sample by equilibration at 348 mV produces an MCD spectrum with little evidence of ferrous hemes b_{558}, b_{595} or *d*. Also absent from the spectrum are bands from oxo-ferryl and ferrous-oxy heme *d*.

Thus, the clean conversion of 'as prepared' oxygenated cytochrome *bd* to its all ferric state is performed and monitored by MOTTLE. Presumably, electrodic reduction and re-oxidation in the absence of oxygen has been accompanied by reduction and release of the oxygen species previously bound to the active site. Such processes may form part of the catalytic cycle in cytochrome *bd*.

5 Perspectives

The examples above illustrate how complementary electronic and structural information may be accessed through spectroelectrochemistry. We have focused here on studies of diffusing proteins. Our current research aims to extend these methods to study adsorbed, functional protein 'films'. Such a configuration offers a number of advantages [26]. Equilibration times are no longer determined by the relatively slow process of protein diffusion. Trivially, this will ensure rapid sample equilibration and facilitate spectroscopic interrogation of a wide potential window. More significantly this approach should allow access to inter- and intra-protein electron

transfer kinetics in a 'pulse-chase' scenario. Application of a potential step would trigger electron transfer. Movement of the electron would be documented by electrical current and time-resolved spectroscopy. We also anticipate being able to assess the response to chemical changes in the protein's environment with appropriately designed flow cells. With these tools in hand we hope to be able to study protein redox chemistry at the molecular level with resolution in the electrochemical potential, time and concentration domains.

Acknowledgments We thank BBSRC (grants C007808 and B15211), the Wellcome Trust (050709) and a JIF award (062178) for financial support of this work.

References

1. Page CC, Moser CC, Dutton PL (2003) Curr Opin Chem Biol 7:551–556
2. Koder RL, Dutton PL (2006) Dalton Trans 3045–3051
3. Vincent KA, Armstrong F (2005) Inorg Chem 44:798–809
4. Armstrong FA (2005) Curr Opin Chem Biol 9:110–117
5. Heering HA, Wiertz FGM, Dekker C, de Vries S (2004) J Am Chem Soc 126:11103–11112
6. Haas AS, Pilloud DL, Reddy KS, Babcock GT, Moser CC, Blasie JK, Dutton PL (2001) J Phys Chem B 105:11351–11362
7. Gregory KB, Bond DR, Lovley DR (2004) Environ Microbiol 6:596–604
8. Jeuken LJC, Connell SD, Henderson PJF, Gennis RB, Evans SD, Bushby R J (2006) J Am Chem Soc 128:1711–1716
9. Angove HC, Cole JA, Richardson DJ, Butt JN (2002) J Biol Chem 277:23374–23381
10. Anderson LJ, Richardson DJ, Butt JN (2001) Biochemistry 40:11294–11307
11. Gwyer JD, Richardson DJ, Butt JN (2004) Biochemistry 43:15086–15094
12. Appia-Ayme C, Little PJ, Matsumoto Y, Leech A P, Berks BC (2001) J Bacteriol 183:6107–6118
13. Moss D, Nabedryk E, Breton J, Mantele W (1990) Eur J Biochem 187:565–572
14. Marritt S, van Wonderen J, Cheesman MR, Butt JN (2006) Anal Biochem 359:79–83
15. Kurkin S, George SJ, Thorneley RNF, Albracht SPJ (2004) Biochemistry 43:6820–6831
16. Bertini I, Cavallaro G, Rosato A (2006) Chem Rev 106:90–115
17. Ambler R P (1991) Biochim Biophys Acta 1058:42–47
18. Yoshida MT, Masuda SN, Nagashima KVP, Vermeglio A, Shimada K, Matsuura K (2001) Biochim Biophys Acta 1506:23–30
19. Berghuis AM, Brayer GD (1992) J Mol Biol 223:959–976
20. Gourion-Arsiquaud S, Chevance S, Bouyer P, Garnier L, Montillet JL, Bondon A, Berthomieu C (2005) Biochemistry 44:8652–8663
21. Ataka K, Heberle J (2004) J Am Chem Soc 126:9445–9457
22. Junemann S (1997) Biochim Biophys Acta 1321:107–127
23. Thomson AJ, Cheesman MR, George SJ (1993) Metallobiochemi C 226:199–232
24. Gadsby PMA, Thomson AJ (1990) J Am Chem Soc 112: 5003–5011
25. Kirk ML, Peariso K (2003) Curr Opin Chem Biol 7:220–227
26. Murgida DH, Hildebrandt P (2005) Phys Chem Chem Phys 7:3773–3784